Laboratory investigation on circular aperture geogrids reinforced soil interface properties

Jie Gu, Mengxi Zhang & Guichao Li
Department of Civil Engineering, Shanghai University, China

ABSTRACT: Geogrids, the most common geosynthetic material, has been widely used to strengthen and protect the structure, and enhance the overall stability of the soil. This paper presented a new reinforcement method by using HDPE circular aperture geogrids. To evaluate the properties of new circular aperture geogrid, a series of large-scale direct shear tests and pull-out tests were conducted on the circular aperture geogrids as well as biaxial geogrids (rectangular aperture). Further, comparative analysis of test results between the two kinds of geogrids was carried out. Based on the large-scale direct shear tests, the relationship between the local shear stress and the displacement of the reinforced soil was studied. Meanwhile the pull-out stress-displacement behaviors of geogrid-soil interface were studied through the large-scale pull-out tests. Both results of two laboratory tests reflected that the circular aperture geogrids performed better than the biaxial geogrids. At the same mesh size, circular aperture geogrid could contribute more geogrid-aggregate interlock affection than rectangular aperture geogrid. As the result, geogrid-soil interface strength was greatly improved. Moreover, residual resistance was determined on the basis of the test results. The results also showed that circular aperture geogrids preformed higher and more stable residual resistance than the biaxial geogrids.

Keywords: Circular aperture geogrids, Direct shear tests, Pull-out tests, Geogrid-soil interface strength, Residual resistance

1 INTRODUCTION

Geogrid, the most common geosynthetic material, is widely used to reinforce retaining walls, as well as subbase or subsoil below roads or structures. Soil pulls apart under tension, while the geogrids are strong in tension. This fact allows the bearing capacity and overall stability of soil structures to be enhanced by geogrids (Huang & Tatsuoka 1990; Bathurst et al. 2006; Li et al. 2008). As a kind of reinforcement buried in the soil mass and gallet, geogrids can not only improve their stability but also reduce their settlement (Palmeira 2004). Nowadays, the study on geogrid-soil interface properties is a major research direction. By conducting laboratory investigation, such as large-scale direct shear tests and pull-out tests, a large number of scholars both home and abroad developed an understanding of interface behaviors of the reinforcement layers (Palmeira 2004; Juran et al. 2010). Large-scale direct shear tests and pull-out tests can also be carried out to model the practical engineering for determining certain engineering design parameters (Liu & Zhou 2009).

Moraci and Recalcati (2006) studied on the factors influencing the geogrid-reinforcement effect and evaluated the apparent friction, peak and residual pull-out resistance. Yang et al. (2006) investigated on influence of different kinds of fills on the interface performances. Moraci and GioffrÈ (2006) presented a new theoretical method to measure the peak and the residual pull-out resistance of extruded geogrids embedded in compacted granular soil. Zhang et al. (2008) proposed a new concept of three-dimensional reinforcement. Dong et al. (2010) studied on the performance of geogrids with triangular apertures under static load. Mosallanezhad (2008; 2016) used a kind of anchoring block with dimensions of 10mm×10mm×10mm to enhance the geogrids. Ezzein and Bathurst (2014) introduced a new-type pull-

out box with a transparent glass-bottom and non-contact measurement device. Zhou et al. (2017) conducted pull-out tests of triangular apertures geogrids and rectangular apertures geogrids. In conclusion, the frictional characteristics of soil-geogrid interface had been extensively studied. However, the influence of the opening shape, especially of circular apertures, hadn't yet been well understood.

The main purpose of this paper was to analyze the influence of different aperture shapes on geogrid-soil interaction. The large-scale direct shear test and pull-out test were carried out to demonstrate the differences between the circular aperture geogrid and conventional rectangular geogrid. According to the shear stress-strain responses, the interface behavior (such as strength and residual pull-out resistance) for two types of geogrids could be analyzed. On this basis, the experiments of circular geogrids with different mesh size were performed for the further study on the friction characteristics of geogrid-soil interface.

2 EXPERIMENTAL STUDIES

2.1 *Apparatus and Instrumentation*

2.1.1 *Pull-out test*

Figure 1 showed the arrangement of the pull-out test. A cube tank with inner dimensions of 300mm×300mm×300mm (L×W×H) was fabricated from 5 aluminum plates and 1 transparent Plexiglas plate. These thick aluminum plates were rigid enough to avoid leading to large deformation of the tank. Through the transparent Plexiglas plate, the displacement of the soil grains could be observed. A slot with dimensions of 10mm×280mm was constructed at the middle of the left part to enable the geogrid to be pulled out of the box.

The vertical load was applied on the loading plate by an oil pump-jack. The horizontal pull-out force, applied by a motor speed reduction device, was speed-controlled. The pull-out speed of 1mm/min was kept avoiding too much influence of the rate of displacement on shear properties. The pull-out displacement was recorded by a resistance displacement sensor which was installed perpendicularly on the profile of the clamp. The pull-out force was applied on the geogrid through the clamp. A load cell was screwed and fixed behind the rigid aluminum clamp to monitor the pull-out force.

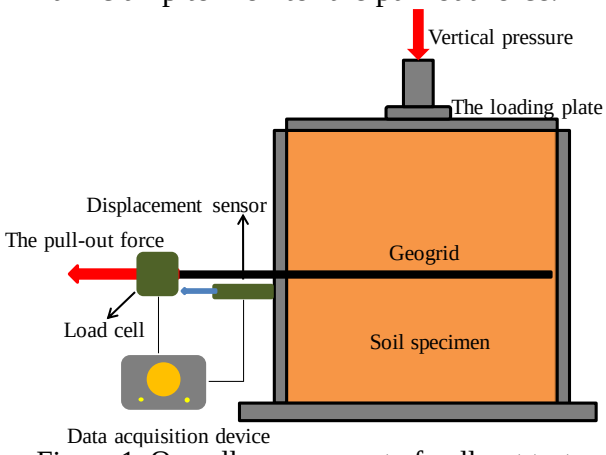

Figure 1. Overall arrangement of pull-out test

2.1.2 *Direct shear test*

Figure 2(a-b) showed front view and vertical view of the large-scale direct shear test respectively. In general, the laboratory test apparatus consisted of an upper box with dimensions of 300mm×250mm×150mm (L×W×H) and a lower box with dimensions of 300mm×300mm×150mm. The width of the upper box was smaller than that of the lower box, aimed to keep a relative constant shear surface area during the tests. The vertical load acting on the loading plate was applied by the oil pump-jack. The shear displacement was applied on the lower box at a constant speed of 1mm/min. The resistance displacement sensor was installed perpendicularly on the left side of the lower box to obtain the actual shear displacement. A high-rigidity force-sensor was fixed on the right of the upper box not only to constrain its horizontal displacement but also monitor the interactive force (shear force: F_s). Assuming the shear stress (τ_s) on the soil-geogrid interface was uniform, the shear stress could be calculated by Eq.(1):

$$\tau_s = F_s/(L \cdot B) \tag{1}$$

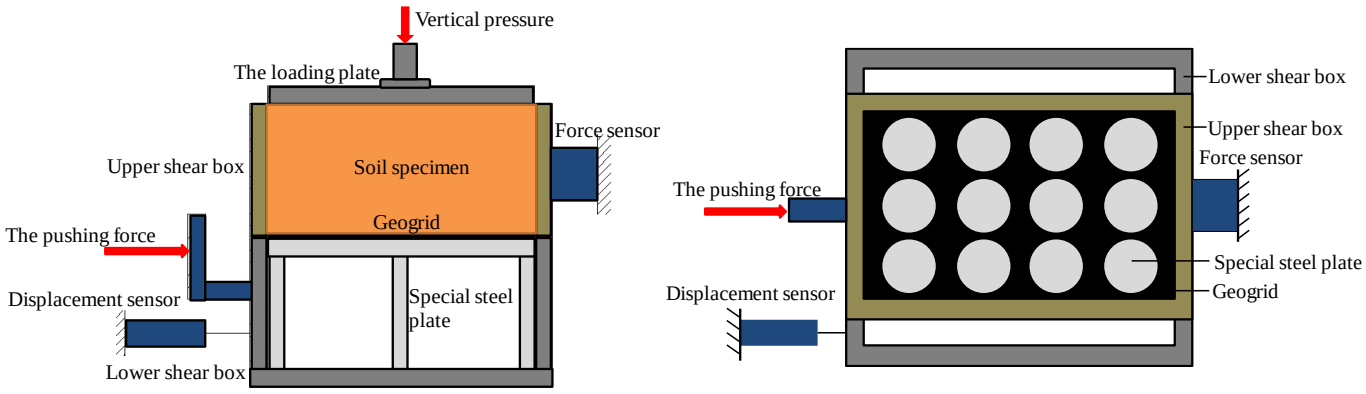

(a) Front view (b) Vertical view

Figure 2. Arrangement of large-scale direct shear test

2.2 *Experimental material*

Geogrids used in the laboratory tests were made of high-density polyethylene (HDPE). The HDPE was processed into different shaped geogrids of 3 mm thickness. The geometry was sketched and the dimension parameters were marked in Figure 3. The values of the dimension parameters were listed in Table 1.

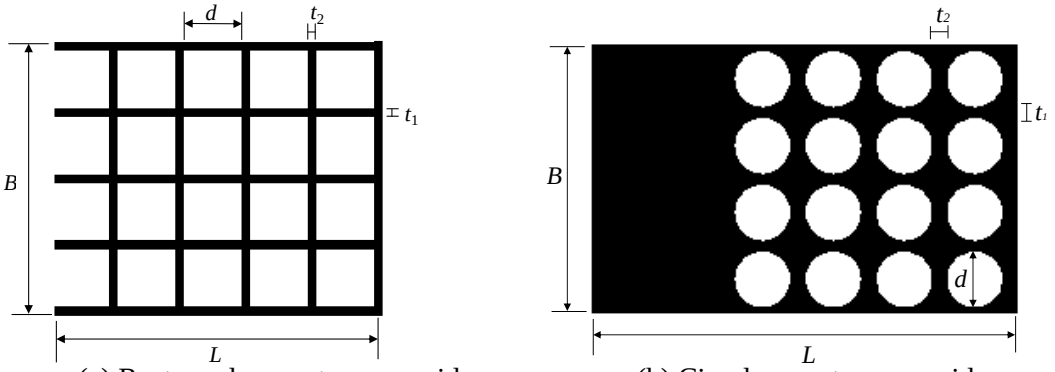

(a) Rectangular aperture geogrid (b) Circular aperture geogrid

Figure 3. Geometry and dimension parameters of geogrids

Table 1. The dimensions of the geogrids

Pull-out test	*B*/mm	*L*/mm	*S*/mm	*t*1/mm	*t*2/mm	*α*
Rectangular aperture	280	450	50	9	9	0.366
Circular aperture	280	450	64	4	11	0.371
			48	18	27	0.596
Direct test	*B*/mm	*L*/mm	*S*/mm	*t*1/mm	*t*2/mm	*α*
Rectangular aperture	240	270	50	9	9	0.337
Circular aperture	240	270	64	12	3	0.366
			48	24	15	0.605

* Where the effective area ratio: $\alpha = \dfrac{(B-t_1)(L-t_2)-S}{(B-t_1)(L-t_2)}$; S is the area of apertures.

The biaxial geogrid (rectangular aperture geogrid) was manufactured through cold drawn technology and enhanced with the ultrasonic welded nodes. Two kinds of circular apertures geogrids were handmade using a simple electric knife to cut out circles from thin HDPE plate. Both type geogrids were made of the same materials and almost had the same tensile strength. The main property parameters of the geogrid were listed in Table 2.

Table 2. The main properties of the geogrid

Tensile yield strength (kN/m)	Tensile strength at 2 % strain (kN/m)	Tensile strength at 5% strain (kN/m)	Yield elongation (%)
30.5	10.2	13.1	13.4

Figure 4 depicted grain size distribution curve and listed the main property parameters of the standard sand. The tests were conducted at a uniform relative density (ID) of 85%. In this test, the relative density was controlled by compaction. The relative density could be controlled as long as the mass of the sand was weighed correctly, for the volume of the tank box was constant, where the mass (m_{sand}) of the sand was calculated by the following Eq.(2):

$$m_{sand} = L \times W \times H \times [(\rho_{max} - \rho_{min}) \times 0.85 + \rho_{min}] = 24.39\text{kg} \quad (2)$$

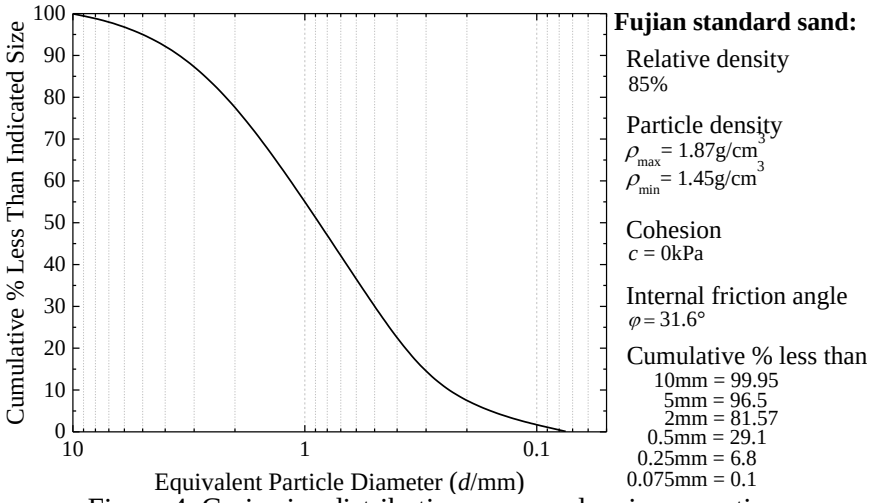

Figure 4**.** Grain size distribution curve and main properties

3 EXPERIMENTAL PROCEDURE AND PROGRAM

3.1 *Pull-out test*

Firstly, the test tank was half filled with clean dry sand. It was noted that the shear surface must be flush with the pull-out-slot, which enabled the geogrids to be pulled out smoothly. The width of the geogrid was 280mm shorter than the width of the tank, remaining 10mm gap on each side to avoid the influence of boundary on the test results. Furthermore, the test tank was filled. After leveling the top-surface of soil specimen, the loading plate was centered on the tank. The vertical pressure, acting on the loading plate, increased slowly to the needed magnitude to prevent the soil mass failure under sudden high loading. After the vertical displacement was stable, the motor speed reduction device started working. The geogrids were pulling out at speed of 1mm/min; meanwhile the horizontal displacement and pull-out force (F_p) were monitored. Assuming the shear stress (τ_p) on the soil-geogrid interface was uniform, the shear stress could be calculated by Eq.(3):

$$\tau_p = F_p/(L \cdot B) \quad (3)$$

Table 3**.** Program of the pull-out test

Number	Identifier	Geogrid type	Vertical pressure (kPa)
1	R-100	Rectangle	100
2	R-150	Rectangle	150
3	R-200	Rectangle	200
4	C64-100	Circle-64	100
5	C64-150	Circle-64	150
6	C64-200	Circle-64	200
7	C48-100	Circle-48	100
8	C48-150	Circle-48	150
9	C48-200	Circle-48	200

*Where Rectangle represented rectangular aperture geogrid; Circle-64 represented circular aperture geogrid with diameter of 64mm; Circle-48 represented circular aperture geogrid with diameter of 48mm.

Table 3 summarized the experimental program. Each test must be repeated 3 times at least and the average values of the good results were finally taken.

3.2 *Direct shear test*

At the beginning, the special steel plate was installed in the lower box. Using epoxy resins, the geogrid was bonded to the steel plate. Then, the upper box was putted on the lower box and filled with sand. After leveling the top-surface of the filler, the loading plate was centered on the upper box. Similar to the pull-out test, three kinds of geogrids were prepared. A series of direct shear tests were conducted under different vertical pressures. Table 4 summarized the experimental program.

Table 4. Program of the direct test

Number	Identifier	Geogrid type	Vertical pressure (kPa)
1	R-100	Rectangle	100
2	R-200	Rectangle	200
3	R-300	Rectangle	300
4	C64-100	Circle-64	100
5	C64-200	Circle-64	200
6	C64-300	Circle-64	300
7	C48-100	Circle-48	100
8	C48-200	Circle-48	200
9	C48-300	Circle-48	300

4 TEST RESULTS AND ANALYSIS

4.1 *Pull-out test*

Figure 5(b-d) showed the comparison of the pull-out stress versus displacement. Obvious non-linear characteristic of the curves was observed. The pull-out stress peak value increased significantly with the increase of vertical pressure. Shear displacement of soil-geogrid interface would cause the soil swelling. However, the soil swelling was confined by the surrounding stable soil, which exerted more additional normal stress. It was the additional normal stress that caused the increment of pull-out stress. It was much in evidence that the higher vertical pressure could cause more normal confinement.

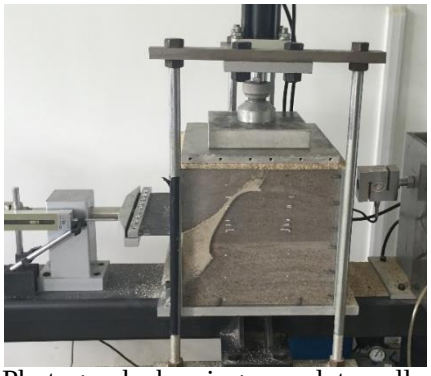

(a) Photograph showing complete pull-out test

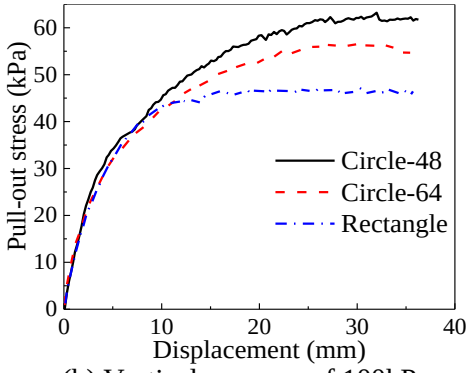

(b) Vertical pressure of 100kPa

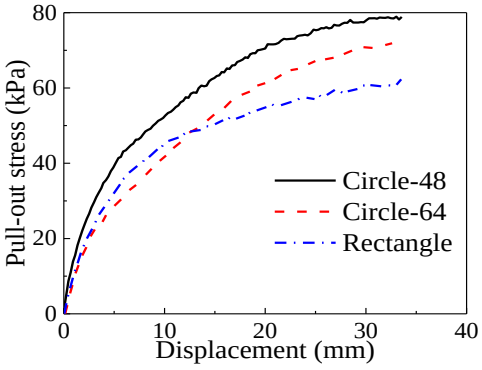

(c) Vertical pressure of 150kPa

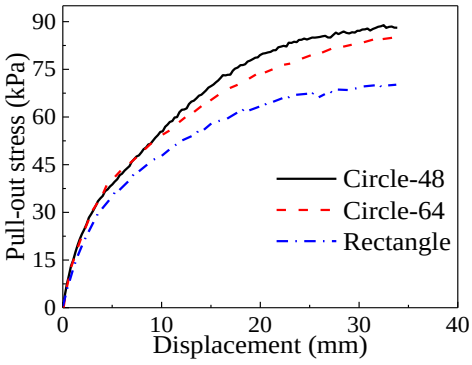

(d) Vertical pressure of 200kPa

Figure 5. Pull-out stress versus vertical pressure curves

The sequence of pull-out stress peak values from high to low was: Circle-48, Circle-64 and Rectangle. Geogrids with higher effective area ratio could contribute more constraining stress on soil, which leaded to higher frictional resistance. It was concluded that circular aperture geogrids could contribute higher constraining stress, comparing with rectangular aperture geogrids.

During the pull-out tests, after the peak values of pull-out stress was observed, the corresponding failure would occur, and the pull-out stress would turn to be the residual values progressively. In the cases, pull-out stress would tend to be stable and not be affected by the increase of displacement. The corresponding residual resistances were listed in Table 5. For different types of geogrid, the coefficients of residual resistance were determined. Coefficients of residual resistance versus vertical pressure curves were depicted in Figure 6. Comparing with rectangular aperture geogrid, the higher coefficients of residual resistance were noted in the case of circular aperture geogrids. The maximum were observed in Circle-48. It was noted that the coefficients of residual resistance decreased with the vertical pressure increased.

Table 5. Residual resistance at different vertical pressure

Vertical pressure/kPa	Geogrid type		
	Circle-48	Circle-64	Rectangle
100	61.6	73.1	90.8
150	54.0	69.8	83.0
200	46.2	60.5	69.2

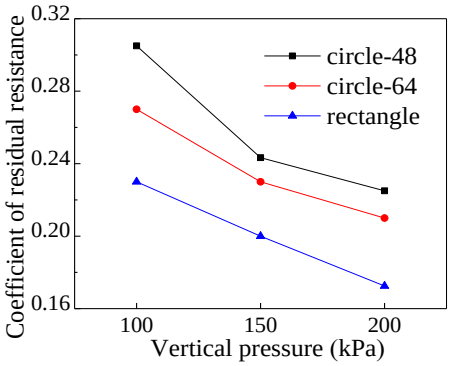

Figure 6. Coefficients of residual resistance

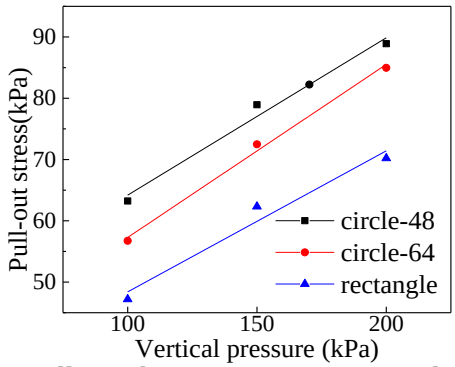

Figure 7. Pull-out shear stress versus vertical pressure curve

* Where the coefficient of residual resistance (η): $\eta = \tau' / 2\sigma$; τ' is the residual resistance; σ is the vertical pressure.

Figure 7 represented the liner fitted curves of peak values, obeying Mohr-Coulomb strength criterion. Based on the fitted curves, two interface parameters, apparent cohesion (c) and apparent internal friction angle (φ) were determined. Table 6 listed the interface parameters of all geogrids. It was found that the circular aperture geogrid had relatively higher interface parameters, comparing to rectangular aperture geogrid. In addition, almost maximum interface parameters were observed in the case of Circle-48 geogrid. It was inferred that circular aperture geogrid could contribute more interlock affection.

Table 6. Interface parameters

Interface property	Geogrid type		
	Circle-48	Circle-64	Rectangle
c/kPa	38.5	29.0	25.4
φ/°	14.4	15.8	13.0

4.2 *Direct shear test*

Direct shear test is generally used to model the sliding failure of reinforcement layer, whose mechanism is quite different from that of pull-out test. The comparison of shear stress-displacement curves under different vertical pressure was showed in Figure 8. There were many differences being observed.

At the vertical pressure of 100kPa, the sequence of shear stress peak values from high to low was Circle-48, Circle-64 and Rectangle. However, almost same value of residual resistances of all the cases was observed. It was indicated that geogrids with higher effective area ratio could contribute higher frictional resistance, but not contribute higher residual resistance. At the vertical pressure of 200kPa, the similar sequence of shear stress peak values was noted too. However the law of the residual resistance looked differently. The C48-200 performed the highest residual resistances, while C64-200 and

R-200 performed the almost same residual resistances still. At the vertical pressure of 300kPa, the C48-300 and C64-300 performed the higher residual resistances than that of R-300. The highest value was observed at C48-300.

(a) Photograph showing complete pull-out test

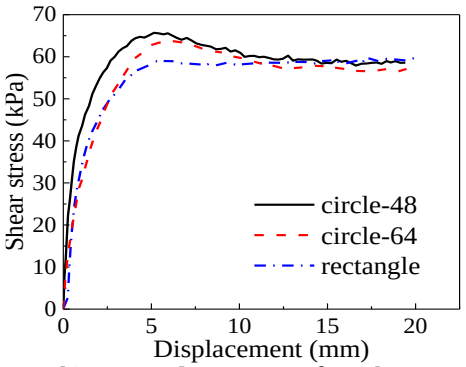

(b) Vertical pressure of 100kPa

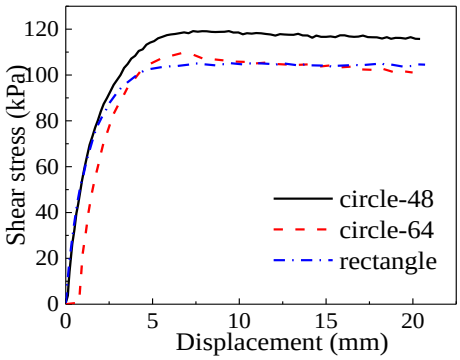

(c) Vertical pressure of 200kPa

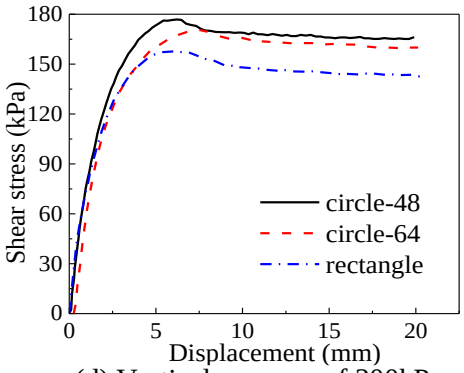

(d) Vertical pressure of 300kPa

Figure 8. Results of the direct shear tests

Figure 9 represented the liner fitted curves of shear-stress peak values and two interface parameters were determined. Table 7 listed the interface parameters of all geogrids. It was found that Circle-48 geogrid possessed relatively higher interface parameters. In addition, the maximum value of apparent internal friction angle was observed in Circle-48.

Table 7. Interface parameters

Interface property	Geogrid type		
	Circle-48	Circle-64	Rectangle
c/kPa	9.4	8.6	9.7
φ/°	29.1	28.0	26.2

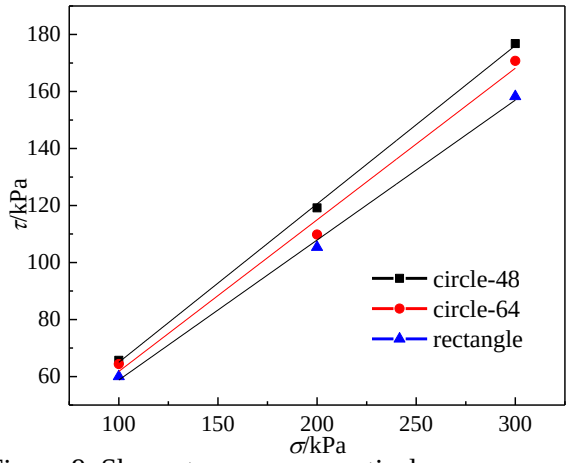

Figure 9. Shear stress versus vertical pressure curve

5 CONCLUSION

This paper presented a series of laboratory investigations on pull-out test and large-scale direct test. The results indicated that:

(a) In pull-out test, circular aperture geogrid exerted higher pull-out stress and residual resistance than that rectangular aperture geogrid. Furthermore, geogrids with higher effective area ratio could contribute higher pull-out stress as well as residual resistance.

(b) In direct shear test, geogrids with higher effective area ratio could contribute higher frictional resistance and perform obviously higher residual resistance under relative high vertical pressure.

(c) In pull-out test, circular aperture geogrid performed higher value of apparent cohesion. Meanwhile, in direct shear test, circular aperture geogrid could perform higher value of apparent internal friction angle. It was concluded that circular aperture geogrid could contribute more geogrid-aggregate interlock affection.

(d) In any case, the circular aperture geogrids preformed higher and more stable residual resistance than the biaxial geogrids.

ACKNOWLEDGMENTS

This study has been supported by the National Natural Science Foundation of China (NSFC) (No. 41372280). The authors would like to express their gratitude for these financial assistances.

REFERENCES

Bathurst, R.J., Vlachopoulos, N., & Walters, D. 2006. The influence of facing stiffness on the performance of two geosynthetic reinforce soil retaining walls. Canadian Geotechnical Journal, Vol. 43(12), pp. 1225-1237.

Dong, Y.L., Han, J., & Bai, X.H. 2010. Behavior of triaxial geogrid-reinforced bases under static loading. Proc. 9th Intl. Conference on Geosynthetics, IFAI, Brazil, pp. 1547-1550.

Dong, Y.L., Han, J., & Bai, X.H. 2011. Numerical analysis of tensile behavior of geogrids with rectangular and triangular apertures. Geotextiles & Geomembranes, Vol. 29(2), pp. 83-91.

Ezzein, F.M. & Bathurst, R.J. 2014. A new approach to evaluate soil-geosynthetic interaction using a novel pullout test apparatus and transparent granular soil. Geotextiles & Geomembranes, Vol. 42(3), pp. 246-255.

Huang, C.C. & Tatsuoka, F. 1990. Bearing capacity of reinforced horizontal sandy ground. Geotextiles & Geomembranes, Vol. 9(1), pp. 51-82.

Juran, I., Guermazi, A., Chen, C.L., et al. 2010. Modelling and simulation of load transfer in reinforced soils: Part 1. International Journal for Numerical & Analytical Methods in Geomechanics, Vol. 12(2), pp. 141-155.

Li, Z.Q., Hu, R.L., Fu, W., et al. 2008. Study on using geogrids to reinforce embankment of expressway. Rock and Soil Mechanics, Vol. 29(3), pp. 795-799.

Liu, W.B. & Zhou, J. 2009. Experimental research on interface friction of geogrids and soil. Rock and Soil Mechanics, Vol. 30(4), pp.965-970.

Moraci, N. & Gioffrè, D. 2006. A simple method to evaluate the pullout resistance of extruded geogrids embedded in a compacted granular soil. Geotextiles & Geomembranes, Vol. 24(2), pp. 116-128.

Moraci, N. & Recalcati, P. 2006. Factors affecting the pullout behaviour of extruded geogrids embedded in a compacted granular soil. Geotextiles & Geomembranes, Vol. 24(4), pp. 220-242.

Mosallanezhad, M., Hataf, N., & Ghahramani, A. 2008. Experimental study of bearing capacity of granular soils, reinforced with innovative grid-anchor system. Geotechnical & Geological Engineering, Vol. 26(3), pp. 299-312.

Mosallanezhad, M., Taghavi, S.H.S., Hataf, N., et al. 2016. Experimental and numerical studies of the performance of the new reinforcement system under pull-out conditions. Geotextiles & Geomembranes, Vol. 44(1), pp. 70-80.

Palmeira, E.M. 2004. Bearing force mobilisation in pull-out tests on geogrids. Geotextiles & Geomembranes, Vol. 22(6), pp. 481-509.

Yang, G.Q., Li, G.X., & Zhang, B.X. 2006. Experimental studies on interface friction characteristics of geogrids. Chinese Journal of Geotechnical Engineering, Vol. 28(8), pp. 948-952.

Yang, Y., Liu, S.Y., & Deng Y.F. 2009. Effect of reinforced subgrade on differential settlement by model test research. Rock and Soil Mechanics, Vol. 30(3), pp. 703-706+711.

Zhang, M.X., Zhou, H., Javadi, A.A., et al. 2008. Experimental and theoretical investigation of strength of soil reinforced with multi-layer horizontal–vertical orthogonal elements. Geotextiles & Geomembranes, Vol. 26(3), pp. 1-13.

Zhou, Y.J., Zheng, J.J., Cao, W.Z., et al. 2017. Experiment study of interface characteristics of different aperture shapes of geogrids reinforced soil. Journal of Southwest Jiaotong University, Vol. 52(3), pp. 482-488.